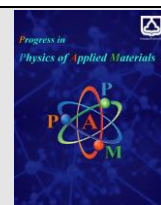




Semnan University

journal homepage: <https://ppam.semnan.ac.ir/>

# Erbium doped Barium Tungstate-Chitosan Nanocomposite: Luminescent Properties

Sanaz Alamdari<sup>1,\*</sup>, Mohammad Hemmati<sup>2</sup>, Majid Jafar Tafreshi<sup>2\*\*</sup>, Mohammad Hossein Ehsani<sup>2</sup><sup>1</sup>Department of Nanotechnology, Semnan University, Semnan, Iran P.O. Box: 35131-19111<sup>2</sup>Faculty of Physics, Semnan University, P.O. Box:35195-363, Semnan, Iran

## ARTICLE INFO

Article history:

Received: 16 September 2023

Revised: 26 October 2023

Accepted: 18 November 2023

Keywords:

Luminescence properties

Nanocomposites

Chitosan

Doping

## ABSTRACT

Recently, there has been an increase in the ability to adjust the optical band gap and enhance the brightness of luminescence in nanophosphors that are used in light-emitting diodes and detectors. In this study, a flexible nanocomposite of erbium-doped barium tungstate (BaWO<sub>4</sub>:Er-1at.%) thin film was synthesized via co-precipitation method, and the structural and luminescence properties were investigated. The effect of excitation wavelength ( $\lambda_{ex}$ ) was studied on the optical properties of the synthesized composite at room temperature. Doped nanocomposite showed the best visible emission in the blue-green range at excitation wavelength ( $\lambda_{ex}=250$ ) of a xenon lamp and a strong violet emission under 980 nm laser excitation. The XRD results verified the presence of BWO, in the chitosan composite structure. FESEM images showed that the prepared hybrid nanocomposite's surface was smooth, consistent, and compact; The Er:BWO particles exhibited a flower-like morphology. These findings demonstrate the potential for employing this nanocomposite in the fabrication of high-performance optoelectronic devices.

## 1. Introduction

Given the outstanding luminescent characteristics of nanomaterials doped with lanthanides, they find utility across a broad spectrum of domains including sensing, photocatalysis, solar cells, bio-imaging, therapy, diagnostics, anti-counterfeiting, latent fingerprint development, optical amplifiers, and solid-state lighting [1-6]. The exploration of luminescent properties in nanomaterials, coupled with an in-depth investigation of their underlying mechanisms, represents an ongoing and pivotal scientific pursuit. This quest arises from the immense potential these materials hold, spanning fundamental physics research to groundbreaking advancements in optoelectronics applications [1]. Within this intriguing realm, researchers have achieved laser emission through both one-photon and two-photon excitation processes within solid matrices infused with dyes. These composite materials have showcased remarkable slope efficiencies, attaining unprecedented

levels of performance. The key to the success of solid-state dye lasers lies in their ability to maintain photostability and mechanical integrity. In this context, chemically derived composite films outshine their organic counterparts, offering superior photostability, optical excellence, and mechanical durability. Solid-state dye lasers prove their practicality in scenarios where low laser output suffices, paving the way for applications such as photodynamic therapy (PDT), laser-induced fluorescence (LIF) in medical tissue diagnostics, and the photodynamic purification of blood to eliminate viruses. The optical characteristics of this material can be altered by introducing different elements through doping or by blending various compounds [5]. The captivating optical phenomenon known as excitation-dependent photoluminescence (EDF), characterized by varying fluorescence based on the excitation source, has garnered significant attention [7]. Despite numerous proposed mechanisms, the precise origin of excitation-dependent photoluminescence remains elusive. Understanding the self-assembly of phospholipids and its

\* Corresponding author. Tel.: +989371803556

E-mail address: [s.alamdari@semnan.ac.ir](mailto:s.alamdari@semnan.ac.ir)

### Cite this article as:

Alamdari S., Hemmati M., Jafar Tafreshi M., Ehsani M.H., 2023. Erbium doped Barium Tungstate-Chitosan Nanocomposite: Luminescent Properties.

*Progress in Physics of Applied Materials*, 3(2), pp. 119-123. DOI: [10.22075/PPAM.2023.31808.1065](https://doi.org/10.22075/PPAM.2023.31808.1065)© 2023 The Author(s). Journal of Progress in Physics of Applied Materials published by Semnan University Press. This is an open access article under the CC-BY 4.0 license. (<https://creativecommons.org/licenses/by/4.0/>)

role in shaping spherical organelles stands as a crucial area of investigation within molecular cell biology. Recent research has demonstrated that erbium-doped lead tungstate/Ag-doped zinc oxide nanocomposite showed strong emission in the blue-green range compared to pure sample at  $\sim\lambda_{ex}=270\text{-}280\text{ nm}$  under UV excitation [8]. Another study highlights that in the prepared ZnO/epoxy films, as the excitation wavelength increased, the photoluminescence peaks exhibited a slight redshift. This phenomenon can be attributed to Kasha's rule and the red edge effect (REE) [5]. This kind of excitation wavelength dependent PL emission behavior appears to be in violation of Kasha's rule of excitation wavelength independence of the emission spectrum of CdO nanoparticles [9]. Recently, dopamine and sodium borohydride were utilized as carbon/nitrogen and boron sources, respectively, in the synthesis process of carbon quantum dots (CQDs); These CQDs exhibited an intriguing excitation-dependent emission behavior and achieved an impressive high quantum yield (QY) of 25%, the highest reported [10]. Recent advancements have enabled the precise tuning of optical band gaps and the enhancement of luminescence in nanophosphors, which find applications in light-emitting diodes and detectors. In this study, we synthesized a flexible nanocomposite thin film of erbium-doped barium tungstate using the co-precipitation method and conducted a thorough investigation of its structural and luminescent properties. Our primary aim is to explore the impact of excitation wavelength ( $\lambda_{ex}$ ) on the optical behavior of this composite at room temperature. The findings are elucidated and discussed primarily in the context of visible emissions.

## 2. Experimental details and Characterizations

High-purity chemicals were used, including Barium nitrate ( $\text{Ba}(\text{NO}_3)_2$ ), erbium III nitrate ( $\text{Er}(\text{NO}_3)_3$ ), sodium tungstate dihydrate ( $\text{Na}_2\text{WO}_4$ ), acetic acid ( $\text{CH}_3\text{COOH}$ ), and Sodium Tripolyphosphate ( $\text{Na}_5\text{P}_3\text{O}_{10}$ ) from Sigma (99.9% purity). To create pure and Er doped  $\text{BaWO}_4$  powder, it was employed a co-precipitation method [11]. To initiate the process, equimolar amounts (0.02 mol) of sodium tungstate and barium nitrate were dissolved in distilled water at room temperature. This solution was then mixed with the barium nitrate solution under ambient conditions. In order to produce doped barium tungstate (BWO), a solution containing sodium tungstate, and erbium III nitrate at a concentration of 1 atomic percent, was carefully added drop by drop to a solution of barium nitrate. The precipitate underwent a drying process followed by calcination at a temperature of  $600\text{ }^\circ\text{C}$ . A brief schematic of experimental works for production of Er:  $\text{BaWO}_4$ -CS thin film is shown in figure 1.

The transformation of chitin into chitosan involved a series of steps, including demineralization, discoloration, deproteinization, and deacetylation [10]. We mixed the synthesized powders (1 gr) with a (3gr) chitosan solution in 100 ml of 1% acetic acid for 1 hour using a mechanical stirrer. Subsequently, we added 1 ml of TPP solution dropwise to the stirring solution. The resulting mixture was then placed on aluminum foils and dried. The flexible layers were separated from the foil after drying.

XRD investigations were conducted using a Bruker D8 diffractometer with  $\text{Cu K}\alpha$  ( $\lambda = 1.54\text{ \AA}$ ). FESEM images provided insights into nanoparticle shape was carried out using a MIRA3TESCAN. Room-temperature PL measurement was performed by Varian Cary Eclipse fluorescence and Up conversion process of the flexible film under a red laser ( $\text{He-Ne } \lambda_{ex} = 632.8\text{ nm}$ ) was applied.

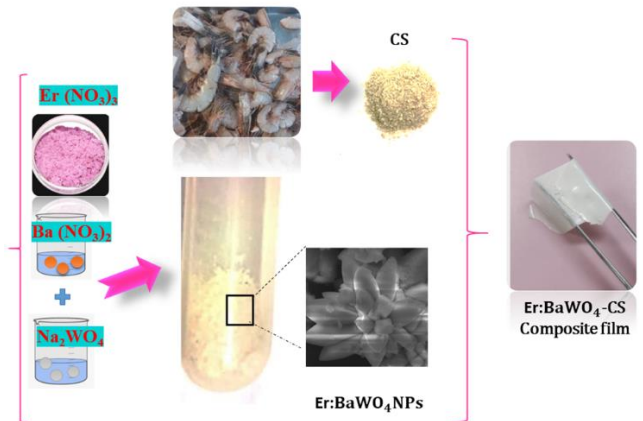
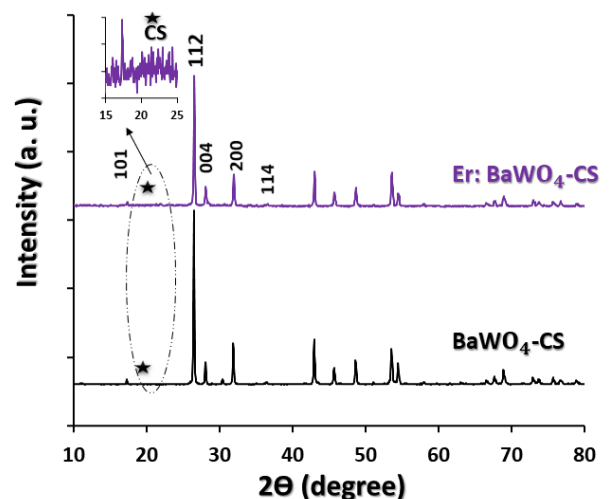


Fig. 1. Brief schematic of experimental works for production of Er:  $\text{BaWO}_4$ -CS thin film.

## 3. Results and discussion

Fig. 2, presents the XRD patterns for pure BWO-CS and Er: BWO-CS films. The discerned diffraction patterns corresponding to BWO align with the scheelite-type tetragonal crystal structure of  $\text{BaWO}_4$ , characterized by the  $I41/a$  (88) space group (JCPDS 43-0646). The peaks at  $2\theta = 20^\circ$  can be attributed to the hydrated and anhydrous structures of chitosan matrix. To estimate the average size of nanocrystals, the Scherrer formula by considering three peaks with the highest intensities has been utilized ( $D=0.9\lambda/\beta\cos\theta$ ) [11]. The resulting calculated average crystallite size for BWO and Er: BWO nanoparticles were approximately 17.5 and 36.6 nm, respectively. By Er doping the intensity of XRD peaks decrease a little and shifted to higher values of  $2\theta$  which could be attributed to atomic radii difference between host and dopant and means the host material is contracting.



**Fig. 2.** XRD patterns of the prepared BWO-CS and BWO: Er-1 at. %-CS thin films.

FESEM images were used to examine the morphology of the prepared hybrid nanocomposite. As is observed in the Figure 3(a, b), the film's surface was smooth, consistent, and compact. The Er: BWO particles exhibited a flower-like morphology.

Fig. 4 show the PL spectra of Er: BWO-CS nanocomposite film with various  $\lambda_{ex}$ =250, 280, 320 and 325 nm (PL Xenon lamp). A change in the shape of the emission spectra with the various energy excitations is observed which is related to the emission bands with a different ratio upon excitation. It should be pointed out that excitations higher than 250 nm are not suitable and possible 4f-4f transitions in dopants or native defects of BWO cannot compete with the incoming energy. The best properties of luminescence were obtained for an excitation wavelength of around 250 nm, in which excitons can be

produced and charge carriers transfers from active intrinsic and extrinsic defect centers can be activated. The produced nanocomposite exhibited a strong green emission band due to  $^4I_{15/2} - ^4F_{7/2}$  transitions in energy levels from  $Er^{+3}$  ion.

Figure 5 shows the photoluminescence decay spectrum of the composite sample. The photoluminescence decay of prepared samples was examined with exponential fits using equation 1 [26,27]:

$$I = \sum_i \alpha_i \exp(-t/\tau_i) \quad (1)$$

Here  $i$  denotes the number of exponentials,  $\tau_i$  and  $\alpha_i$  denote the lifetime and the preexponential factor, respectively, for each component. The photoluminescence decay spectrum of the Er: BWO-CS sample have been monitored at ambient temperature to calculate the exciton lifetime. And it was estimated as  $\tau = 253 \mu s$ .

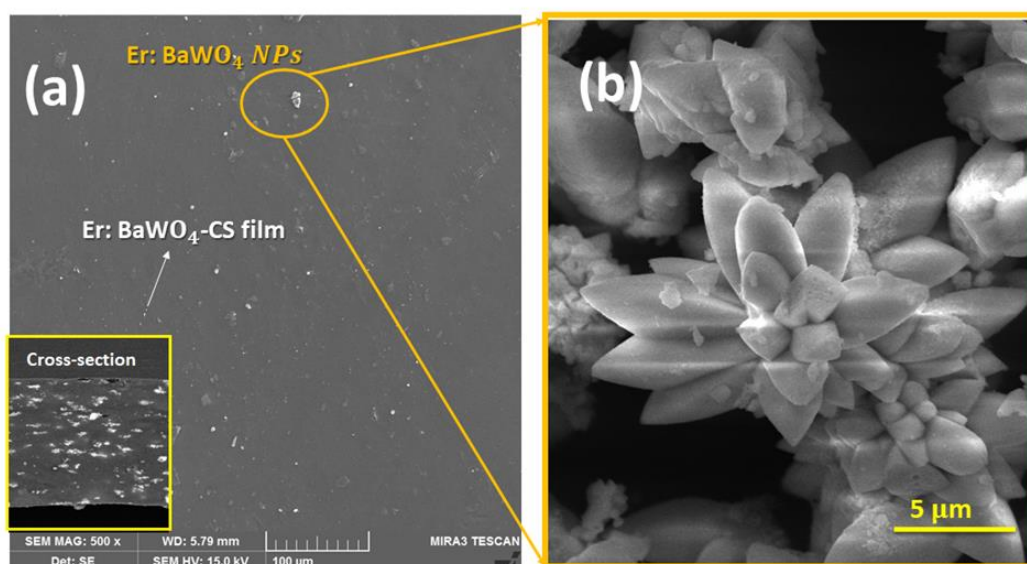


**Fig. 3.** (a) FESEM image of surface of the Erbium doped Barium Tungstate-Chitosan nanocomposite thin film and (b) Erbium doped Barium Tungstate nanopowders

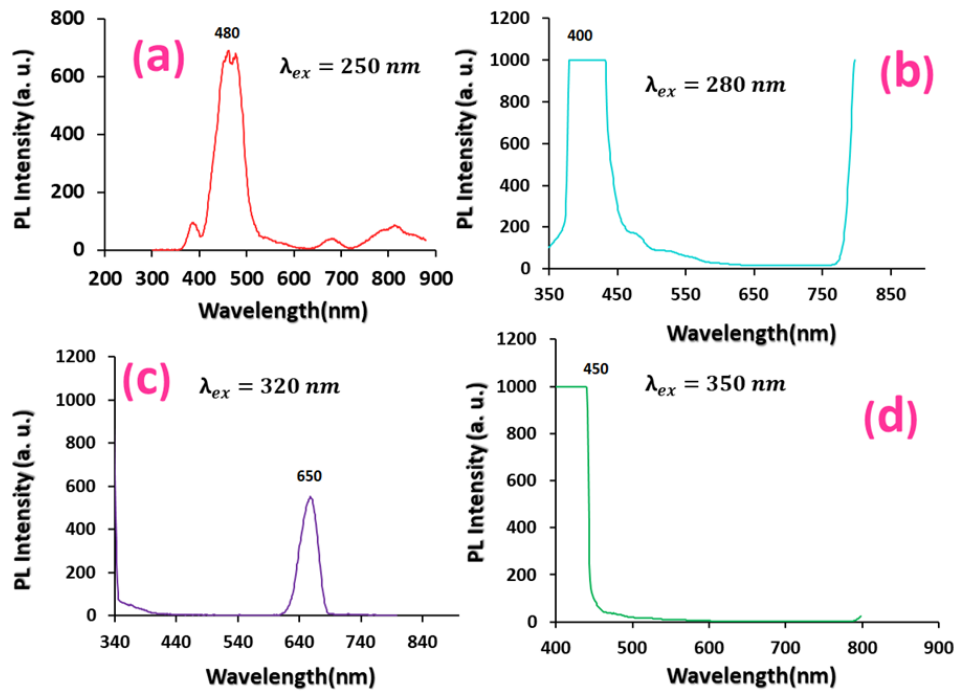


Fig. 4. PL spectra of the Erbium doped Barium Tungstate-Chitosan nanocomposite thin film with various excitation wavelengths of a xenon lamp at room temperature.

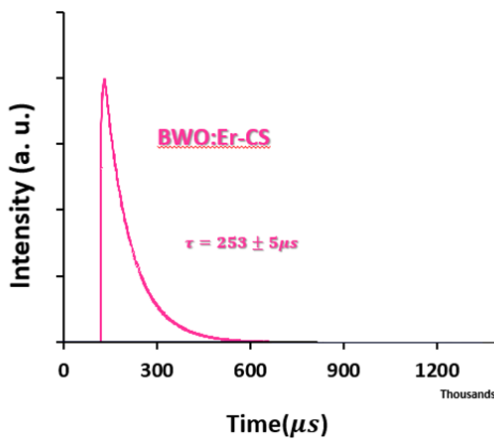


Fig. 5. Photoluminescence decay spectrum of the prepared sample.

Luminescence spectra of neat CS and Er: BWO-CS nanocomposites were studied using the 980 nm laser as an alternative excitation source, as illustrated in Figure 6. It was found that prepared Er: BWO-CS nanocomposite showed strong violet emission when compared to neat CS. Lanthanides possess a multitude of valence electron energy levels and microstates [12,13]. Erbium, exhibits various types of transitions, encompassing sharp 4f-4f intra-configurational transitions, broader 4f-5d transitions, and charge transfer transitions. The process begins with the initial excitation of an electronic transition within one of the nanoparticles. This is followed by the capture of charges at the dopant sites. Subsequently, there is a recombination of electron-hole pairs at these captured sites. This process serves to populate the luminescent energy levels of the dopant, as illustrated in Figure 6. Consequently, achieving the finest and most effective luminous properties in composite phosphors hinges on the strategic utilization of band gap engineering and selecting the optimal excitation energy [14]. In an indirect excitation

mechanism, achieved by the combination of activated ions with opposite parity configuration from the surrounding crystal lattice, may boost the emission efficiency; The probability of 4f intra-shell transitions is often influenced by the specific ionic species that surround the  $\text{Er}^{+3}$  ion [15,16]. Blue emissions are assigned to  ${}^2\text{G}(1)_{9/2} \rightarrow {}^4\text{I}_{15/2}$  and  ${}^3\text{T}_{1u} \rightarrow {}^1\text{A}_{1g}$ , the emission peaks around 500 nm are attributed to the  $\text{T}_{2u} \rightarrow \text{T}_{2g}$  and  ${}^2\text{H}_{11/2} \rightarrow {}^4\text{I}_{15/2}$  transitions and emission peaks around 640 nm are related to  ${}^4\text{F}_{9/2} \rightarrow {}^4\text{I}_{15/2}$  transitions in tungstate groups and  $\text{Er}^{+3}$  ions [15,16].

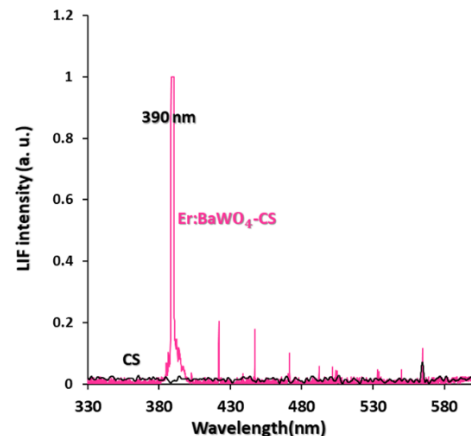


Fig. 6. Luminescence spectra of neat CS and Erbium doped Barium Tungstate-Chitosan nanocomposite thin film under 980 nm laser excitation source at room temperature.

#### 4. Conclusion

A flexible nanocomposite of erbium-doped barium tungstate ( $\text{BaWO}_4$ : Er-1at. %) thin film was synthesized via co-precipitation method. The effect of excitation wavelengths/sources on the luminescent characteristics of the prepared nanocomposites was studied. The prepared nanocomposites exhibited strong blue-green emission

band, indicating that the strength of visible photoluminescence emissions could be controlled by modifying the excitation wavelength. Notably, a more intense luminescence was observed when the excitation wavelength selected around 250 nm. When an alternative excitation source, the 980 nm laser, was employed, the prepared Er: BWO-CS nanocomposite displayed a distinct violet emission in contrast to neat CS. Erbium, exhibited various types of transitions, radiative levels/defects, and charge transfer transitions in BWO matrix. This outcome holds significance in discerning which of the active dopants is more effectively stimulated by the utilized pump source. These findings demonstrate the potential for employing this approach in the creation of high-performance optoelectronic devices.

### Acknowledgements

The authors would like to acknowledge the support extended by the Ahmadi Roshan project of the National Elite Foundation.

### Conflicts of Interest

The author declares that there is no conflict of interest regarding the publication of this article.

### Reference

- [1] Shen, X.B., Song, B., Fang, B., Jiang, A.R., Ji, S.J. and He, Y., 2018. Excitation-wavelength-dependent photoluminescence of silicon nanoparticles enabled by adjustment of surface ligands. *Chemical Communications*, 54(39), pp.4947-4950.
- [2] Mansourian, M. and Alamdari, S., 2023. Fabrication and Investigation on Luminescence Properties of Bi<sub>2</sub>WO<sub>6</sub> Microfibers via Stretching Process. *Progress in Physics of Applied Materials*, pp.1-5.
- [3] Alamdari, S., Haji Ebrahimi, M., Mirzaee, O., Jafar Tafreshi, M., Majlesara, M.H., Tajali, M., Sasani Ghamsari, M. and Mohammadi, A., 2022. Cerium doped Tungsten-Based Compounds for Thermoluminescence Application. *Progress in Physics of Applied Materials*, 2(1), pp.35-40.
- [4] Alamdari, S., Ghamsari, M.S., Afarideh, H., Mohammadi, A., Geranmayeh, S., Tafreshi, M.J. and Ehsani, M.H., 2019. Preparation and characterization of GO-ZnO nanocomposite for UV detection application. *Optical Materials*, 92, pp.243-250.
- [5] Hosseinpour, M., Mirzaee, O., Alamdari, S., Menéndez, J.L. and Abdoos, H., 2023. Novel PWO/ZnO heterostructured nanocomposites: Synthesis, characterization, and photocatalytic performance. *Journal of Environmental Management*, 345, p.118586.
- [6] Ghamsari, M.S., Alamdari, S., Razzaghi, D. and Pirlar, M.A., 2019. ZnO nanocrystals with narrow-band blue emission. *Journal of Luminescence*, 205, pp.508-518.
- [7] Lee, K.M., Cheng, W.Y., Chen, C.Y., Shyue, J.J., Nieh, C.C., Chou, C.F., Lee, J.R., Lee, Y.Y., Cheng, C.Y., Chang, S.Y. and Yang, T.C., 2013. Excitation-dependent visible fluorescence in decameric nanoparticles with monoacylglycerol cluster chromophores. *Nature Communications*, 4(1), p.1544.
- [8] Hosseinpour, M., Abdoos, H., Alamdari, S., Mirzaee, O. and Menéndez, J.L., 2023. Lead Tungstate/Zinc Oxide Heterostructure Nanocomposites: Luminescent Properties Under UV/Red Laser Excitation. *Journal of Composites and Compounds*, 5(15), pp.70-73.
- [9] Thomas, P. and Abraham, K.E., 2015. Excitation wavelength dependent visible photoluminescence of CdO nanomorphotypes. *Journal of Luminescence*, 158, pp.422-427.
- [10] Karadag, S.N., Ustun, O., Yilmaz, A. and Yilmaz, M., 2022. The fabrication of excitation-dependent fluorescence boron/nitrogen co-doped carbon quantum dots and their employment in bioimaging. *Chemical Physics*, 562, p.111678.
- [11] Hemmati, M., Tafreshi, M.J., Ehsani, M.H. and Alamdari, S., 2022. Highly sensitive and wide-range flexible sensor based on hybrid BaWO<sub>4</sub>@ CS nanocomposite. *Ceramics International*, 48(18), pp.26508-26518.
- [12] Han, Y., Gao, C., Wei, T., Zhang, K., Jiang, Z., Zhou, J., Xu, M., Yin, L., Song, F. and Huang, L., 2022. Modulating the Rise and Decay Dynamics of Upconversion Luminescence through Controlling Excitations. *Angewandte Chemie*, 134(45), p.e202212089.
- [13] Debnath, G.H., Mukherjee, P. and Waldeck, D.H., 2020. Optimizing the key variables to generate host sensitized lanthanide doped semiconductor nanoparticle luminophores. *The Journal of Physical Chemistry C*, 124(49), pp.26495-26517.
- [14] Zhdachevskyy, Y., Hizhnyi, Y., Nedilko, S.G., Kudryavtseva, I., Pankratov, V., Stasiv, V., Vasylechko, L., Sugak, D., Lushchik, A., Berkowski, M. and Suchocki, A., 2021. Band gap engineering and trap depths of intrinsic point defects in ralo<sub>3</sub> (r= y, la, gd, yb, lu) perovskites. *The Journal of Physical Chemistry C*, 125(48), pp.26698-26710.
- [15] Yang, F., Tu, C., Li, J., Jia, G., Wang, H., Wei, Y., You, Z., Zhu, Z., Wang, Y. and Lu, X., 2007. Growth and optical property of ZnWO<sub>4</sub>: Er<sup>3+</sup> crystal. *Journal of luminescence*, 126(2), pp.623-628.
- [16] Gao, D., Zhang, X., Zheng, H., Gao, W. and He, E., 2013. Yb<sup>3+</sup>/Er<sup>3+</sup> codoped β-NaYF<sub>4</sub> microrods: Synthesis and tuning of multicolor upconversion. *Journal of alloys and compounds*, 554, pp.395-399.